

## Quantum rotation of carbonyl sulfide molecules in superfluid helium clusters: a path integral hybrid Monte Carlo study

This article has been downloaded from IOPscience. Please scroll down to see the full text article.

2005 J. Phys.: Condens. Matter 17 S3259

(<http://iopscience.iop.org/0953-8984/17/45/010>)

View [the table of contents for this issue](#), or go to the [journal homepage](#) for more

Download details:

IP Address: 129.252.86.83

The article was downloaded on 28/05/2010 at 06:40

Please note that [terms and conditions apply](#).

# Quantum rotation of carbonyl sulfide molecules in superfluid helium clusters: a path integral hybrid Monte Carlo study

**Shinichi Miura**

Institute for Molecular Science, 38 Myodaiji, Okazaki 444-8585, Japan

E-mail: [miura@ims.ac.jp](mailto:miura@ims.ac.jp)

Received 16 September 2005

Published 28 October 2005

Online at [stacks.iop.org/JPhysCM/17/S3259](http://stacks.iop.org/JPhysCM/17/S3259)

## Abstract

Carbonyl sulfide (OCS) molecules in superfluid helium-4 clusters have been studied by path integral hybrid Monte Carlo methods. A new technique was developed to treat the quantum rotational degree of freedom of the molecules in hybrid Monte Carlo methods; this is referred to as a ‘Legendre potential technique’. Then, our method was applied to OCS-doped helium clusters. It was found that although the molecule is solvated inside the cluster, the calculated orientational correlation function exhibits free-rotor-type behaviour. The estimated effective rotational constant was in good agreement with the experimental value.

(Some figures in this article are in colour only in the electronic version)

## 1. Introduction

Chemical processes in condensed helium-4 have recently been shown to exhibit various exotic properties due to superfluidity of the medium [1]. An impressive example is provided by carbonyl sulfide (OCS) molecules dissolved in helium nanodroplets [1]. The infrared spectrum of the OCS molecules inside  $^4\text{He}$  (boson) and  $^3\text{He}$  (fermion) droplets has been measured. For the  $^4\text{He}$  droplets, sharp rotational lines were observed, whereas for the  $^3\text{He}$  droplets only a broad line was found. The former behaviour implies that molecules rotate freely in the droplets; the latter may be qualitatively understood in terms of conventional rotational diffusion in the solution. Since the intermolecular interactions are virtually identical for the two systems, the difference between the spectra originates from the difference in quantum statistics between the two systems. The helium-4 droplets at the state point investigated are expected to be in a superfluid state [2] characterized by vanishing ‘viscosity’; thus, the free-rotor behaviour can be attributed to the superfluidity at a molecular level. This example indicates that the macroscopic quantum phenomena such as superfluidity have dramatic effects on the microscopic processes in the quantum medium.

To date, the OCS-doped helium clusters at finite temperature have been theoretically studied by path integral Monte Carlo methods [3]. In that study, the rotational fluctuation of the molecules could not be directly accessed, since the OCS molecule was treated as a classical object fixed at the origin. In the present study, we have extended our path integral hybrid Monte Carlo method [4] to treat quantum rotation of the molecules. Then, the method was applied to the OCS-doped helium clusters to probe the quantum rotational fluctuation of the solvated molecules.

## 2. Method

We consider a system consisting of  $N$  helium-4 atoms obeying Bose–Einstein statistics and an OCS molecule modelled as a rigid rotor. The partition function of the system  $Z$  at an inverse temperature  $\beta = 1/k_B T$  is written in discretized path integral form as [2, 5]

$$Z = \frac{1}{N!} \sum_{\mathcal{P}} \int \cdots \int \prod_{s=1}^M d\mathbf{R}^{(s)} d\Omega^{(s)} \prod_{s=1}^M \rho(\mathbf{R}^{(s)}, \Omega^{(s)}, \mathbf{R}^{(s+1)}, \Omega^{(s+1)}; \Delta\tau) \quad (1)$$

where  $\Delta\tau = \beta/M$  is the imaginary time step and  $\rho(\Delta\tau)$  is the short time (or high temperature) density matrix of the system. Here,  $\mathbf{R}^{(s)}$  denotes the  $3(N+1)$ -dimensional position vector, including the molecule's centre-of-mass position, and  $\Omega^{(s)}$  represents the molecule's orientation in the laboratory frame; the superscript  $s$  runs from 1 to  $M$ , indicating the corresponding imaginary time slice. The permutation  $\mathcal{P}$  is included in the boundary condition of the path:  $\mathbf{R}^{(M+1)} = \mathcal{P}\mathbf{R}^{(1)}$ . In the present study, the He–He contribution in the density matrix is represented using the pair product form of the exact two-body density matrices, and the He molecule contribution is approximated using the standard factorization technique accurate up to  $\mathcal{O}(\Delta\tau^4)$  [5]. In this expression, the rotational density matrix of the molecule is included as [5]

$$\rho^{\text{rot}}(\Omega^{(s)}, \Omega^{(s+1)}; \Delta\tau) = \sum_{J=0}^{\infty} \frac{2J+1}{4\pi} P_1(\cos\gamma) e^{-\Delta\tau B J(J+1)} \quad (2)$$

where  $P_1$  is a Legendre function and  $\gamma$  is an angle between the molecular axes of two successive time slices. The parameter  $B$  is the rotational constant of the molecule related to the moment of inertia  $I$ ,  $B = \hbar^2/2I$ . In order to incorporate the molecular rotation in the hybrid Monte Carlo algorithm, we define the following ‘potential function’ using the rotational density matrix:  $\rho^{\text{rot}}(\Delta\tau) \equiv e^{-\Delta\tau W^{\text{rot}}(\Omega, \Omega')}$ . We refer to  $W^{\text{rot}}$  as a ‘Legendre potential of rotation’. In the hybrid Monte Carlo case, an equation of motion is needed to generate trial configurations. We introduce a fictitious angular momentum and a fictitious moment of inertia to sample rotational fluctuations. Then, we integrate this technique into our hybrid Monte Carlo algorithms for correlated Bose liquids [4]. Further details on the method will be presented elsewhere [6].

## 3. Computational details

The calculated system consists of  $N = 64$  helium-4 atoms and an OCS molecule at temperature 0.37 K. The number of discretizations is chosen to be  $M = 216$ , corresponding to  $1/\Delta\tau = 80$  K. The rotational constant of the OCS molecule is taken from a gas-phase experimental value,  $B = 0.20286 \text{ cm}^{-1}$  [7]. The Aziz potential [8] is used as a pairwise interaction between two helium atoms. The morphed potential of Howson and Hutson [9] is adopted for the He–OCS interaction. Path integral hybrid Monte Carlo calculations are performed for the system obeying Bose–Einstein statistics. For comparison, the system obeying Maxwell–Boltzmann statistics is also examined.

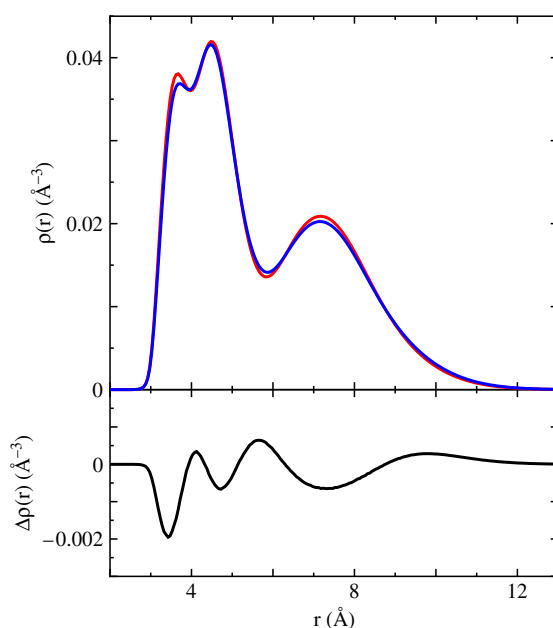


**Figure 1.** Radial density profiles of helium atoms measured from the centre of mass of the OCS molecule (upper panel). The blue line is for the system obeying Bose–Einstein statistics  $\rho_{B-E}(r)$  and the red line for the system obeying Maxwell–Boltzmann statistics  $\rho_{M-B}(r)$ . Difference of the two radial density profiles (lower panel):  $\Delta\rho(r) = \rho_{B-E}(r) - \rho_{M-B}(r)$ .

#### 4. Results

We show the radial density profile of the helium atoms around the centre of mass of the OCS molecule in figure 1. First, we discuss the results on the bosonic cluster. An oscillatory structure of the solvent density is found around the OCS molecule; it indicates that the solvation shell structure is well developed around the molecule. Since the density of the bulk liquid helium is  $\rho = 0.022 \text{ \AA}^{-3}$ , the primary peak is about twice denser than  $\rho$ . A subpeak at  $r = 3.7 \text{ \AA}$  is found in the primary peak. This substructure comes from the minimum of the OCS–helium interaction located near the carbon atom; see figure 2 in [9] for details on the interaction potential. We can define the first solvation shell using the minimum of  $\rho(r)$  at  $r = 5.9 \text{ \AA}$ . The coordination number in the first solvation shell was calculated to be 20.5. As seen in the figure, the difference of the quantum statistics has a minor effect on the density profile. The bosonic exchange of the helium atoms is found to make the density profile broader; the largest effect is around the subpeak at  $r = 3.7 \text{ \AA}$ . Here, we briefly comment on the effect of the Bose statistics on the structure of the helium clusters. As found in radial distribution functions of liquid helium-4 [2], the bosonic exchange has little effect on structural quantities related to the diagonal component of the density matrix. A great effect can be found in properties related to the off-diagonal component including imaginary time correlations. At the end of this section, this will be demonstrated by analysing the orientational fluctuation of the molecule in imaginary time.

It is interesting to decompose the above density profile using the length of exchange cycles among the helium atoms, since the superfluid state of the clusters is characterized by the long exchange cycles, comparable to the system size [2]. We denote the density profile of the helium atoms participating in the exchange cycle with the length  $P$  (for  $P = 1, \dots, 5$ ) as  $\rho^{(P)}(r)$ .

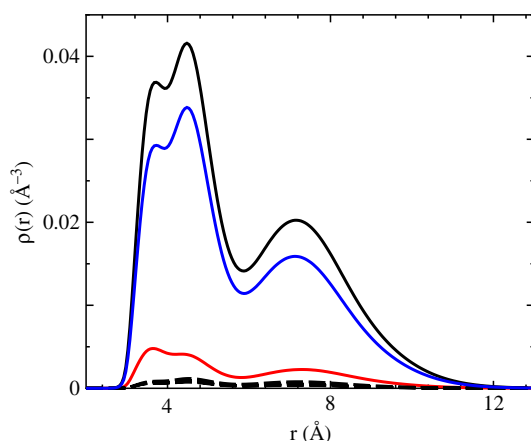


**Figure 2.** Radial density profiles of helium atoms measured from the centre of mass of the OCS molecule. The black solid line is for the total density profile, the blue line for  $\rho^{(6)}(r)$ , and the red line for  $\rho^{(1)}(r)$ . Black dashed lines are for  $\rho^{(P)}(r)$  for  $P = 2, \dots, 5$ . The definition of  $\rho^{(P)}(r)$  is given in the text.

In the case of the superscript  $P = 6$ ,  $\rho^{(6)}$  represents the density profile of the helium atoms participating in the cycle of length  $P \geq 6$ . The decomposed density profile is presented in figure 2. It is found that the total density profile is composed of two major components: one is  $\rho^{(1)}$  and the other is  $\rho^{(6)}$ . The components from short exchange cycles  $P = 2, \dots, 5$  add small contributions to the total density profile. Both components,  $\rho^{(1)}$  and  $\rho^{(6)}$ , have shell structures reflecting the total density profile. According to Kwon *et al* [3], we may regard  $\sum_{P=1}^5 \rho^{(P)}(r)$  as a local disturbance of the superfluidity. As seen in the figure, the dominant contribution of the non-superfluid component is found in the first solvation shell; the highest peak is located at the substructure of the total density profile where the OCS–helium interaction is minimum. The coordination number of the non-superfluid component in the first solvation shell was calculated to be 3.9; then, 19% in the first coordination shell can be assigned to be the non-superfluid component by this definition, and the complementary superfluid component is 81% in the first solvation shell.

Next, we present the results on dynamical correlations of the OCS molecule. First, we show translational motion of the centre of mass of the OCS molecule. The translational correlation is well described by the following mean square correlation function:

$$R^2(\tau) = \langle |\mathbf{r}(\tau) - \mathbf{r}(0)|^2 \rangle \quad (3)$$

where  $\mathbf{r}(\tau)$  denotes the centre-of-mass position of the OCS molecule at an imaginary time  $\tau$ . This correlation function is periodic in  $[0, \beta]$ . The correlation function at  $\tau = \beta/2$  reflects the quantum delocalization of the centre of mass of the molecule. For the free OCS molecule, the correlation function can be expressed analytically [10]:

$$R^2(\tau) = \frac{3\beta\hbar^2}{m} \left[ \frac{\tau}{\beta} \left( 1 - \frac{\tau}{\beta} \right) \right] \quad (4)$$

with  $m$  denoting the total mass of the OCS molecule. The calculated results are presented in figure 3. Since the molecule interacts with surrounding helium atoms, the spatial fluctuation is suppressed compared with that of the free OCS molecule. Interestingly,  $R(\beta/2)$  for the bosonic cluster is larger than that for the Boltzmann-type cluster:  $R(\beta/2) = 0.93 \text{ \AA}$  for the bosonic cluster, and  $0.84 \text{ \AA}$  for the Boltzmann-type cluster. This indicates that the effect of the confinement by the surrounding solvent atoms is weaker in the case of the bosonic cluster.

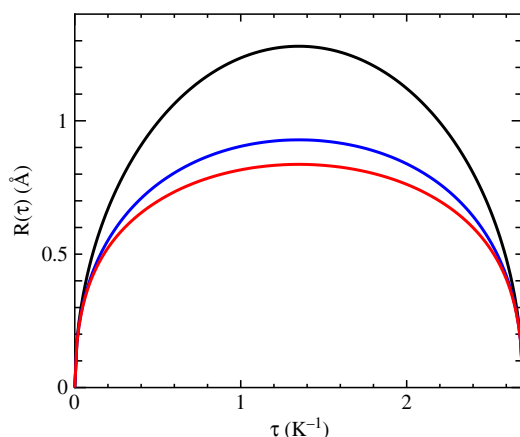


**Figure 3.** Root mean square correlation function  $R(\tau)$  of the centre of mass of the OCS molecule as a function of the imaginary time  $\tau$ . The blue line is for the system obeying Bose–Einstein statistics, the red line for the system obeying Maxwell–Boltzmann statistics, and the black line for the free OCS.

Finally, we present the results regarding the rotational motion of the molecule. The rotational fluctuation can be probed by the following orientational correlation function:

$$C(\tau) = \langle \mathbf{e}(\tau) \cdot \mathbf{e}(0) \rangle \quad (5)$$

where  $\mathbf{e}(\tau)$  is a unit vector proportional to the molecular axis at an imaginary time  $\tau$ . This correlation function is again periodic in the imaginary time. For the free OCS with a rotational constant  $B$ , we can write  $C(\tau)$  in the following analytical form [11]:

$$C(\tau) = \frac{1}{Z} \left\{ e^{-2B\tau} + \sum_{J>0} e^{-\beta BJ(J+1)} \left[ J e^{B2J\tau} + (J+1) e^{-B2(J+1)\tau} \right] \right\} \quad (6)$$

with  $Z = \sum_{J=0}^{\infty} (2J+1) e^{-\beta BJ(J+1)}$ . The calculated correlation functions are shown in figure 4. For comparison, the correlation function for an isolated OCS is also presented, which was calculated using equation (6) with the gas-phase experimental value  $B = 0.20286 \text{ cm}^{-1}$ . As in the translational correlation, the solute–solvent interaction suppresses the orientational fluctuation compared with that for the gas-phase OCS. Unlike the translational motion, however, the bosonic correlation of the solvent helium is found to have large effects on the orientational correlation;  $C(\tau)$  for the bosonic cluster shows qualitatively different behaviour compared with the Boltzmann-type counterpart. Using the correlation function for the bosonic cluster, we estimated an effective rotational constant  $B_{\text{eff}}$  of the solvated OCS in such a way that the value of  $C(\beta/2)$  was fitted to the free-rotor expression, equation (6), at  $\tau = \beta/2$ ; in this procedure,  $B$  was treated as a fitting parameter. The resulting value was  $B_{\text{eff}} = 0.083 \text{ cm}^{-1}$ , which is in good agreement with the experimental value of the nanodroplets  $B_{\text{eff}} = 0.0732 \text{ cm}^{-1}$  [12]. In figure 4, we present the free-rotor correlation function with the estimated  $B_{\text{eff}}$ . We find that  $C(\tau)$  for the solvated OCS in the bosonic cluster is well described by the free-rotor  $C(\tau)$  with  $B_{\text{eff}}$ . This demonstrates that our method realizes the effective free rotation of the OCS molecule in the superfluid cluster.

## 5. Concluding remarks

We have developed path integral hybrid Monte Carlo methods for molecule-doped helium clusters. To handle quantum rotational motion in the algorithm, we introduced a new method

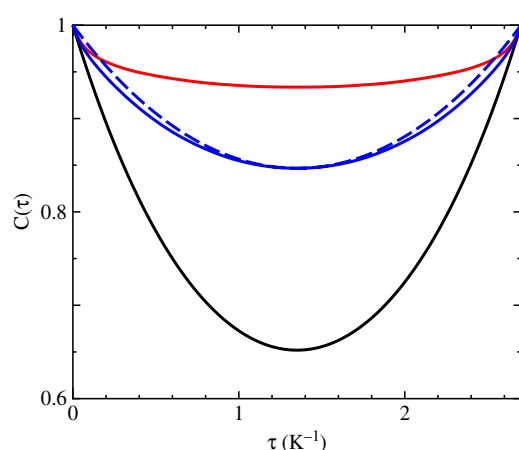


**Figure 4.** Orientational correlation function  $C(\tau)$  of the OCS molecule as a function of the imaginary time  $\tau$ . The blue solid line is for the system obeying Bose–Einstein statistics, the red line for the system obeying Maxwell–Boltzmann statistics, and the black line for the free OCS with the gas-phase rotational constant  $B$ . The blue dashed line is for the correlation function of the free OCS with  $B_{\text{eff}}$  estimated from the value of the bosonic  $C(\beta/2)$ .

called the Legendre potential technique. Then, the experimentally observed effective free rotation of the OCS molecule in superfluid clusters was successfully reproduced. For further study, the calculated rotational constant should be connected to the microscopic solvation structure of the molecule. Although the microscopic superfluid density given by Kwon *et al* [3] provides qualitative features of the quantum solvation, more elaborate estimation of the local superfluid density may be required for quantitative discussion [13]. Detailed analysis on this issue will be presented in the near future.

### Acknowledgments

The author thanks the Research Centre for Computational Science, National Institutes of Natural Sciences, for the use of supercomputers. This work was partially supported by a Grant-in-Aid for Scientific Research (No 15750016) from the Japan Society for the Promotion of Science and by NAREGI Nanoscience Project from the Ministry of Education, Culture, Sports, Science, and Technology, Japan.

### References

- [1] Toennies J P and Vilesov D F 1998 *Annu. Rev. Phys. Chem.* **49** 1 and references therein
- [2] Ceperley D M 1995 *Rev. Mod. Phys.* **67** 279 and references therein
- [3] Kwon Y, Huang P, Patel M V, Blume D and Whaley K B 2000 *J. Chem. Phys.* **113** 6469 and references therein
- [4] Miura S and Tanaka J 2004 *J. Chem. Phys.* **120** 2160
- [5] Marx D and Muser M H 1999 *J. Phys.: Condens. Matter* **11** R117 and references therein
- [6] Miura S 2005 in preparation
- [7] Hunt N, Foster S C, Johns J W C and McKellar A R W 1985 *J. Mol. Spectrosc.* **111** 42
- [8] Aziz R A, Janzen A R and Moldover M 1995 *Phys. Rev. Lett.* **74** 1586
- [9] Howson J M M and Hutson J M 2001 *J. Chem. Phys.* **115** 5059
- [10] Nichols A L III, Chandler D, Singh Y and Richardson D 1984 *J. Chem. Phys.* **81** 5190
- [11] Blinov N, Song X G and Roy P-N 2004 *J. Chem. Phys.* **120** 5916
- [12] Grebenev S, Hartmann M, Havenith M, Sartakov B, Toennies J P and Vilesov A F 2000 *J. Chem. Phys.* **112** 4485
- [13] Draeger E W and Ceperley D M 2003 *Phys. Rev. Lett.* **90** 065301